Frequency-domain ANN Non-linear Active Device Model for Harmonic-Balance-based CAD

Chiara Ramella, Simone Corbellini, Simona Donati Guerrieri, Marco Pirola

Dept. Electronics and Telecommunications, Politenico di Torino, Turin, Italy
chiara.ramella@polito.it

(*Invited Paper*)

***Abstract*—In this work we demonstrate a feed-forward Artificial Neural Network (ANN) model for microwave active devices, here an FET, where the input and outputs are the device harmonic port waves. The ANN has been trained through an in-house tool implementing back-propagation and gradient descent, with load-pull data sweeping the available input power from back-off to harsh compression. The ANN model can be seamlessly used as a replacement of any active device model in microwave CAD tools implementing the Harmonic Balance (HB) algorithm. As a demonstrator, we developed in MATLAB an HB circuit solver implementing the ANN device model within an external circuit simulating the device with different loading conditions. The ANN modeling approach been successfully applied both in class A and a class B bias.**

***Index Terms*—artificial neural networks, harmonic balance, microwave CAD, non-linear device modeling**

I. Introduction

Accurate large-signal modeling of microwave transistors is fundamental to achieve high reliability in the design of power amplifiers and other non-linear microwave circuits. On the other hand, device models should be also computationally efficient to allow for agile design optimization, hence the widespread use of equivalent circuit (compact) models [1], [2]. Recently, behavioral models have gained interest as an effective way to accurately model non-linear devices, starting from measurements [3] or physical simulations [4]. In this scenario, artificial neural networks (ANNs) are promising candidates [5]–[7] as they are capable to fit complicated non-linear power and/or bias dependence with smooth functions: an important feature for the Harmonic Balance (HB) based non-linear simulations, typical of microwave non-linear design.

In the literature, ANNs are often exploited to model DC and AC parameters as a function of bias, temperature or other auxiliary variables [8], [9] or to mimic compact model parameters, e.g. in the ADS DynaFET model [10], also incorporating memory, trap or temperature effects [11]–[13]. Despite the wide literature, few black-box behavioral device models are present [14]–[16], based on port waves in frequency domain. Most of these models focus on power amplification, and assume a linearization around a Large Signal Operating condition (LSOP), where the ANN input is the incident wave amplitude at the fundamental frequency (akin to X-parameters [17]) possibly complemented by the incident wave at the output port (e.g. Cardiff model [18]). In this work, instead, the ANN inputs are all the incident waves at all the harmonics [19], while all the reflected waves are the ANN outputs. Such a model can be seamlessly introduced in any EDA tool implementing the Harmonic Balance (HB) algorithm.

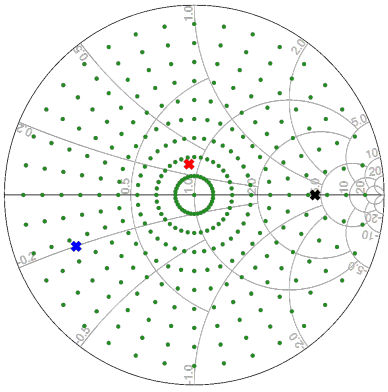

Fig. 1. Fundamental load pull (green dots) considering 10 magnitude values, from 0.1 to 0.9 with 0.1 step, and 36 phase values, from 0° to 350° with 10° step. Crosses are the test loads adopted in Sec IV: $(45 + j20)\,\Omega$ (red), $(10 - j10)\,\Omega$ (blue) and $225\,\Omega$ (black).

In this preliminary work, we address the ANN model of a MESFET device in GaAs technology, modeled in Keysight ADS through a cubic Curtice model, limiting the training data to load-pull at the fundamental frequency. To demonstrate the capability of the ANN model to be used as a replacement of other active device models in HB circuit solvers, avoiding the complexity of its implementation into commercial CAD tools, we have implemented a simple Harmonic Balance solver in MATLAB. The aim is to show that the ANN model can be used with unknown input and output waves, to be determined within a circuit solver, rather that testing it only with surrogate data. We show that HB MATLAB solutions show very good agreement with ADS HB simulations.

The proposed model can be easily generalized to other operating conditions by extending the ANN database for training, e.g. including higher harmonic loads and/or increasing the number of harmonics, harmonic stimuli and bias.

II. Training data generation

In this preliminary work, focused on the methodology, a relatively simple active device has been considered, namely a 500-nm GaAs epitaxial MESFET of 1 mm gate periphery, described though a cubic Curtice model fitting available

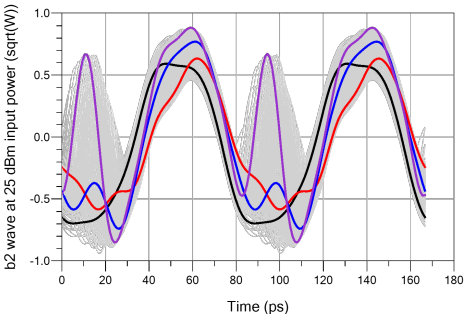

Fig. 2. Example of port wave (b_2) waveforms in compression obtained with load-pull sweeps.

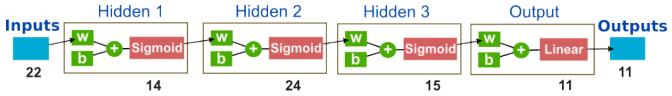

Fig. 3. Structure of the implemented feed-forward network: 64 trainable neurons have been employed, for a total of 1233 parameters.

physical (TCAD) simulation data at 12 GHz [4].

The maximum drain current at 8 V drain supply, is around 355 mA, giving an optimum class-A load resistance around 45 Ω, while an imaginary part in the 10-20 Ω range gives the best trade-off between maximum output power and efficiency [20]. For this work we considered two cases: class A biasing (177 mA quiescent current), and nearly class B biasing (14 mA quiescent current, corresponding to less than 5% class-AB bias point). For both biasing conditions, we considered a fundamental load pull over the entire Smith Chart, as shown in Fig. 1, while the higher output harmonics have been terminated with a short circuit (tuned-load). In all cases, the input source impedance was fixed at 20 Ω at all harmonics: a value deliberately different to the normalization impedance (50 Ω), to force non-zero waves. The input available power was swept from -10 dBm up to 30 dBm, ensuring sufficient gain compression with all loads.

Adopting around 100 of points in the power sweep (non-uniform but finer in compression) for each of the 360 loads considered yields a total of ~ 36 k points. For each point the complex harmonic phasors of the port waves with a $R_0 = 50\ \Omega$ normalization resistance

$$\mathrm{a}_{nh} = \frac{\mathrm{V}_{nh} + R_0 \mathrm{I}_{nh}}{2\sqrt{R_0}}; \quad \mathrm{b}_{nh} = \frac{\mathrm{V}_{nh} - R_0 \mathrm{I}_{nh}}{2\sqrt{R_0}} \tag{1}$$

are computed based on port voltages V_{nh} and currents I_{nh} and are collected for the ANN training and testing. With $H = 5$ harmonics and $N = 2$ ports (gate and drain), the overall dataset includes $36000 \times (2H + 1) \times 2N$ real values. As an example of the port wave data, Fig. 2 reports all the b_2 waveforms at 25 dBm available input power, highlighting four of them to demonstrate the variety of harmonic content that correspond to different loading conditions.

III. Neural Network

Two identical feed-forward neural networks have been used to independently model the reflected waves at the gate and drain ports. By analyzing networks of different sizes and complexity, the best performances have been obtained with a fully connected network with the structure depicted in Fig. 3:

- an input layer of $(2H + 1) \times N = 22$ neurons taking as input the DC and the incident harmonic waves (a, real and imaginary components) at both device ports;
- 3 hidden layers composed respectively by 14, 24 and 15 neurons with a sigmoid activation function and bias input;
- an output layer of $2H + 1 = 11$ neurons, with a linear activation function and bias input, whose outputs represent the DC and the reflected harmonic waves (b, real and imaginary components) at both device ports.

For the training of both the networks, the whole data set has been randomly divided into a training set (80%) and a test set (20%). No data has been reserved for the validation, since the plan is to further evaluate the network performance through the HB simulations, which intrinsically involves the generation of new data. In order to improve the network capability of managing harmonics of different amplitudes, all the real and imaginary components of the network inputs and outputs have been linearly pre-processed to span the range $[-1, +1]$.

The network training has been performed by means of an in-house tool written in C language that provides, with respect to standard solutions, ad-hoc features for the network configuration and training, such as the possibility to manually trim each optimizer's parameter during the training. The tool implements the back-propagation with stochastic gradient descent according to the Adam optimizer. However, in order to speed-up the learning, mini-batches of variable size have been employed, starting from almost an online learning with only two elements up to ten thousand elements. The network performance has been evaluated employing the mean square error between the computed and the target reflected waves (real and imaginary components) for each harmonic, along with the maximum error for each harmonic, to highlight the worst case bound. The complete training of the two ANNs took about 2 hours on a 2.8 GHz I7 CPU for both the class-A and class-B cases.

IV. Harmonic Balance with ANN device model

The simulation environment is described in Fig. 4. The overall device ANN model, given by the combination of the two extracted ANNs, was implemented in MATLAB. It represents a nonlinear multi-port connected with an embedding network, including the harmonic loads and the external sources.

According to the HB technique, the circuit solution is found by imposing the wave continuity for each harmonic. Collecting all the a and b waves in vectors, the HB system reads

$$\mathbf{b}_{\mathrm{ext}} = \mathbf{a}_{\mathrm{NN}} \tag{2}$$

$$\mathbf{a}_{\mathrm{ext}} = \mathbf{b}_{\mathrm{NN}} \tag{3}$$

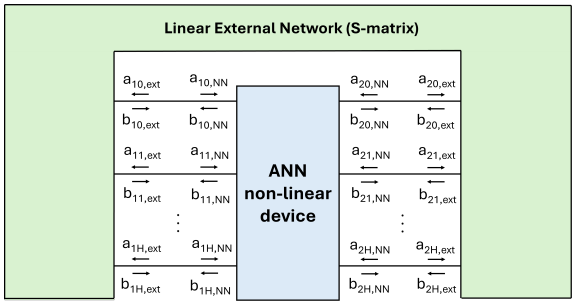

Fig. 4. Harmonic Balance simulation environment implemented in MATLAB: $\mathrm{a(b)}_{nh,\mathrm{ext}}$ and $\mathrm{a(b)}_{nh,\mathrm{NN}}$ are the incident and reflected waves at the n-th port and h-th harmonic of the external and ANN blocks, respectively.

Equations (2) and (3) must be solved for all ports and all harmonics (here 5 + DC) along with the constitutive equations of the two blocks.

The external network is linear and thus can be represented in the frequency domain through its S-parameters plus impressed waves $\mathbf{b}_{0\mathrm{ext}}$ to account for independent sources [4]:

$$\mathbf{b}_{\mathrm{ext}} = \mathbf{S}\,\mathbf{a}_{\mathrm{ext}} + \mathbf{b}_{0\mathrm{ext}} \tag{4}$$

while the ANN model is

$$\mathbf{b}_{\mathrm{NN}} = \mathrm{ANN}(\mathbf{a}_{\mathrm{NN}}) \tag{5}$$

The ANN model has been then expanded by adding auxiliary equations for the output of each layer to keep the jacobian implementation simple. The total number of equations is

$$2N \times (2H+1) + \sum_{l=1}^{L} n_l \tag{6}$$

where N is the number of ports, L the number of layers, n_l the number of neurons in each layer and H the number of harmonics included in the simulation, corresponding to $(2H+1)$ equations for each variable (H complex numbers + DC). With the number of neurons reported in Sec. II, the HB system consists of 150 equations.

The HB solver has been tested with power sweeps on multiple loads, not included in the original dataset used for the ANN training and testing. The loads are presented at the fundamental frequency at the drain port, keeping the input port source at $20\,\Omega$ and the higher drain harmonics shunted. For the device biased in class A, the three loads marked in Fig. 1 are selected as examples of widely different operating condition: high-impedance load (black), capacitive load with low real part (blue) and close to the optimum load (red). The outcome of the simulation with the MATLAB HB solver is presented in Fig. 5, compared to circuit simulations (ADS) solving the same circuit with the original Curtice model. A nearly perfect match is achieved, demonstrating the ANN model accuracy and its ability to be seamlessly included in HB algorithms.

Also for the class-B case, the accuracy is very good, as shown in Fig. 6, where the operation of the device on the optimum load (red cross in Fig. 1) is presented.

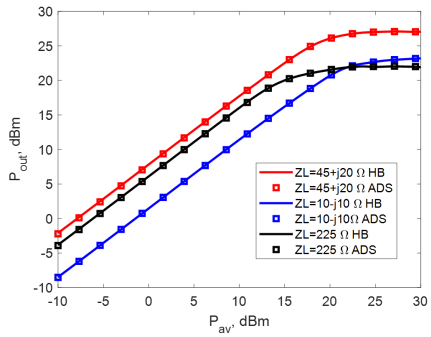

(a) Output power as a function of available input power.

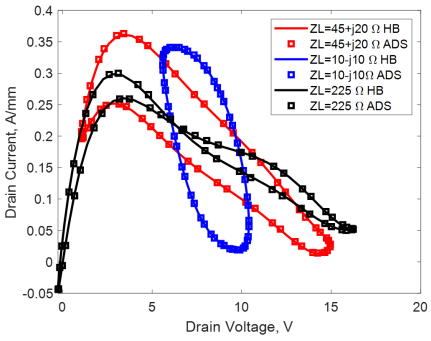

(b) Dynamic load lines at 21.3 dBm available input power.

Fig. 5. HB solution of the class-A stage for different fundamental loads (see Fig. 1): MATLAB HB solution with ANN model (lines) compared to circuit simulation with Curtice model (symbols).

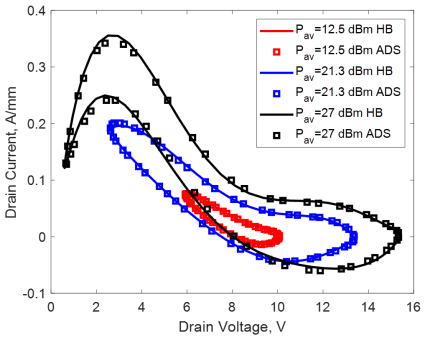

Fig. 6. HB solution of the class-B stage with $(45+j20)\,\Omega$ fundamental load (close to the optimum load): dynamic load lines at different power levels; MATLAB HB solution with ANN model (lines) compared to circuit simulation with Curtice model (symbols).

V. Conclusion

We presented a preliminary black-box ANN model of a GaAs MESFET device, considering all the incident and reflected port waves at all the harmonics as inputs and outputs, respectively. The ANN is extracted with a custom software from load-pull data at the fundamental frequency, while source impedance and output harmonic terminations are kept constant. The proposed ANN model has been exploited within HB simulation, accurately reproducing the device behavior up to deep compression levels.

ACKNOWLEDGMENT

This work was carried out within the "Stacked power architectures for next generation mobile and space communications in European gallium arsenide technology (STARGATE)" project – funded by European Union – Next Generation EU within the PRIN 2022 PNRR program (D.D.1409 del 14/09/2022 Ministero dell'Università e della Ricerca). This manuscript reflects only the authors' views and opinions and the Ministry cannot be considered responsible for them.

REFERENCES

[1] I. Angelov, V. Desmaris, K. Dynefors, P. Nilsson, N. Rorsman, and H. Zirath, "On the large-signal modelling of AlGaN/GaN HEMTs and SiC MESFETs," in *GAAS 2005*, 2005, pp. 309–312.

[2] G. P. Gibiino, A. Santarelli, and F. Filicori, "A GaN HEMT Global Large-Signal Model Including Charge Trapping for Multibias Operation," *IEEE Trans. Microw. Theory Techn.*, vol. 66, no. 11, pp. 4684–4697, 2018.

[3] G. Avolio, A. Raffo, M. Marchetti, G. Bosi, V. Vadalà, and G. Vannini, "GaN FET Load-Pull Data in Circuit Simulators: a Comparative Study," in *EuMIC 2019*, 2019, pp. 80–83.

[4] S. Donati Guerrieri, C. Ramella, E. Catoggio, and F. Bonani, "Bridging the Gap between Physical and Circuit Analysis for Variability-Aware Microwave Design: Modeling Approaches," *El.*, vol. 11, no. 6, 2022.

[5] B. Liu and J. Cai, "Comparative analysis of nonlinear behavioral models for GaN HEMTs based on machine learning techniques," *Int. J. Numer. Model.*, vol. 37, no. 2, p. e3177, 2024.

[6] L. Kouhalvandi and S. Donati Guerrieri, "Modeling of HEMT Devices Through Neural Networks: Headway for Future Remedies," in *ICEEE 2023*, 2023, pp. 261–267.

[7] F. Feng, W. Na, J. Jin, J. Zhang, W. Zhang, and Q.-J. Zhang, "Artificial Neural Networks for Microwave Computer-Aided Design: The State of the Art," *IEEE Trans. Microw. Theory Techn.*, vol. 70, no. 11, pp. 4597–4619, 2022.

[8] A. Jarndal, "On Neural Networks Based Electrothermal Modeling of GaN Devices," *IEEE Access*, vol. 7, pp. 94 205–94 214, 2019.

[9] A. Jarndal, S. Husain, and M. Hashmi, "Genetic algorithm initialized artificial neural network based temperature dependent small-signal modeling technique for GaN high electron mobility transistors," *Int. J. RF Microw. Computer-Aided Eng.*, vol. 31, no. 3, p. e22542, 2021.

[10] J. Xu, R. Jones, S. A. Harris, T. Nielsen, and D. E. Root, "Dynamic FET model - DynaFET - for GaN transistors from NVNA active source injection measurements," in *IMS 2014*, 2014, pp. 1–3.

[11] X. Tang, A. Raffo, N. Donato, G. Crupi, and J. Cai, "Theoretical and Experimental Analysis of a CSWPL Behavioral Model for Microwave GaN Transistors Including DC Bias Voltages," *IEEE Trans. Comput.-Aided Design Integr. Circuits Syst.*, vol. 43, no. 3, pp. 933–943, 2024.

[12] A.-D. Huang, Z. Zhong, W. Wu, and Y.-X. Guo, "An Artificial Neural Network-Based Electrothermal Model for GaN HEMTs With Dynamic Trapping Effects Consideration," *IEEE Trans. Microw. Theory Techn.*, vol. 64, no. 8, pp. 2519–2528, 2016.

[13] W. Hu, H. Luo, X. Yan, and Y.-X. Guo, "An Accurate Neural Network-Based Consistent Gate Charge Model for GaN HEMTs by Refining Intrinsic Capacitances," *IEEE Trans. Microw. Theory Techn.*, vol. 69, no. 7, pp. 3208–3218, 2021.

[14] J. Cai, J. Wang, C. Yu, H. Lu, J. Liu, and L. Sun, "An artificial neural network based nonlinear behavioral model for RF power transistors," in *APMC 2017*, 2017, pp. 600–603.

[15] J. Louro, C. Belchior, D. R. Barros, F. M. Barradas, L. C. Nunes, P. M. Cabral, and J. C. Pedro, "New Transistor Behavioral Model Formulation Suitable for Doherty PA Design," *IEEE Trans. Microw. Theory Techn.*, vol. 69, no. 4, pp. 2138–2147, 2021.

[16] J. Louro, L. C. Nunes, F. M. Barradas, T. R. Cunha, P. M. Cabral, and J. C. Pedro, "A Hammerstein-Like Broadband ANN-Based Transistor Behavioral Model," *IEEE Trans. Microw. Theory Techn.*, vol. 72, no. 6, pp. 3288–3299, 2024.

[17] N. Lei, F. Jiang, and L. Sun, "X-parameter modelling of gan hemt based on neural network," *The Journal of Engineering*, vol. 2019, no. 23, pp. 8955–8958, 2019. [Online]. Available: https://ietresearch.onlinelibrary.wiley.com/doi/abs/10.1049/joe.2018.9156

[18] M. Tian, J. Bell, E. Azad, R. Quaglia, and P. Tasker, "A Novel Cardiff Model Coefficients Extraction Process Based on Artificial Neural Network," in *PAWR 2023*, 2023, pp. 1–3.

[19] L. Kouhalvandi and S. Donati Guerrieri, "Nonlinear Behavioral Modeling of FETs: Toward the Implementation of Deep Neural Networks through Large Signal Data and EDA Tools," in *presented at EuMIC 2024*, 2024.

[20] C. Ramella, S. Donati Guerrieri, and M. Pirola, "TCAD-based Pseudo-Common-Gate X-PAR Model for GaAs Stacked Power Amplifier Design," in *INMMIC 2023*, 2023, pp. 1–4.